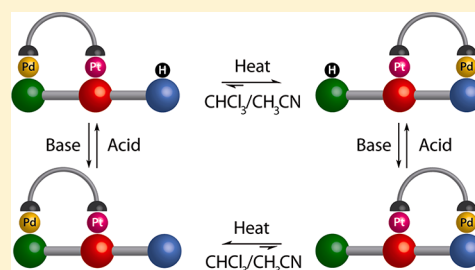


Toward Metal Complexes That Can Directionally Walk Along Tracks: Controlled Stepping of a Molecular Biped with a Palladium(II) Foot

Jonathon E. Beves,[†] Victor Blanco,^{†,‡} Barry A. Blight,[†] Romen Carrillo,[†] Daniel M. D'Souza,[†] David Howgego,[†] David A. Leigh,^{*,†,‡} Alexandra M. Z. Slawin,[§] and Mark D. Symes[†][†]School of Chemistry, University of Edinburgh, The King's Buildings, West Mains Road, Edinburgh EH9 3JJ, United Kingdom[‡]School of Chemistry, University of Manchester, Oxford Road, Manchester M13 9PL, United Kingdom[§]School of Chemistry, University of St. Andrews, Purdie Building, St. Andrews, Fife KY16 9ST, United Kingdom

S Supporting Information

ABSTRACT: We report on the design, synthesis, and operation of a bimetallic molecular biped on a three-foothold track. The “walker” features a palladium(II) complex “foot” that can be selectively stepped between 4-dimethylaminopyridine and pyridine ligand sites on the track via reversible protonation while the walker remains attached to the track throughout by means of a kinetically inert platinum(II) complex foot. The substitution pattern of the three ligand binding sites, together with the kinetic stability of the metal–ligand coordination bonds, affords the two positional isomers a high degree of metastability, meaning that altering the chemical state of the track does not automatically instigate stepping in the absence of an additional stimulus (heat in the presence of a coordinating solvent). The use of metastable metal complexes for foot–track interactions offers a promising alternative to dynamic covalent chemistry for the design of small-molecule synthetic molecular walkers.



1. INTRODUCTION

In the past few years small molecules that are able to “walk” down short tracks have been described,^{1,2} a mode of molecular level transport inspired by the bipedal motor proteins from the myosin, dynein, and kinesin superfamilies.³ The biological systems employ a combination of hydrogen bonding, electrostatic interactions, and hydrophobic binding to attach each foot to the track with only one foot–track attachment labilized at any time so that the walker maintains at least one point of contact with the track at all times during the walking process, leading to processivity of transport. However, designing foot–track binding so that it is locked at one point (when the other foot is “stepping”) but labile when required to step is far from easy, given present-day understandings of how to control noncovalent interactions. Accordingly, many^{1a–c,e–j} of the synthetic small-molecule systems designed thus far utilize dynamic covalent chemistry (which combines the reversibility of supramolecular chemistry with the controllability and robustness of covalent bonding) for the walker–track interactions.

An alternative, potentially highly controllable, means of connecting the feet of a molecular biped to a track could be to employ metal coordination bonding. Although transition-metal coordination motifs have been widely employed as molecular switches and devices⁴ where redox,⁵ chemical,⁶ or photo stimuli⁷ have been used effectively to direct molecular structure and function, there are few examples of using metal–ligand interactions to induce controlled molecular-level motion away from equilibrium. Apart from the use of zinc(II) ions to

instigate conformational change in a single stroke of a rotary motor,^{6d} examples of motor mechanisms involving metal–ligand bonds have been limited to interlocked stimuli-switchable molecular shuttles⁸ in which a thread can be manipulated to translocate a submolecular component energetically uphill and subsequently reset without undoing the task performed.⁹ The manipulation of metal–ligand binding kinetics may facilitate the transportation pathways of ratcheting and escapement in the design of molecular motors. Here we describe a molecular biped that employs a platinum(II) complex as one foot and a palladium(II) complex as the other foot. The palladium(II) foot can be made to step between different ligand sites on the track, pivoting about the kinetically locked platinum(II) foot. The molecular walker can be driven energetically uphill and ultimately fixed into a thermodynamically unfavorable positional isomer distribution without permanently altering the state of the footholds, realizing efficient metal-coordination-mediated stepping of a molecular biped.

2. RESULTS AND DISCUSSION

2.1. Complex Design and Addressability of a Metal-Complex Foot. The metal complexes employed for each foot of the proposed bimetallic molecular walker (Figure 1) are based upon a motif previously used to organize tridentate pyridine-2,6-dicarboxamide and derivatized monodentate pyr-

Received: December 5, 2013

Published: January 14, 2014

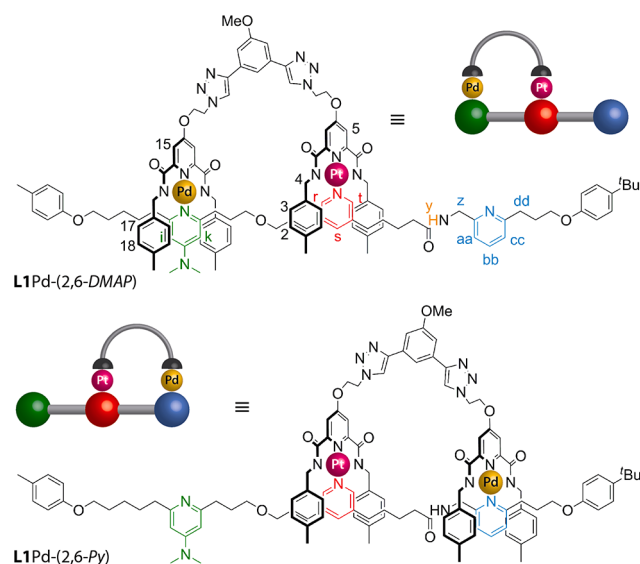


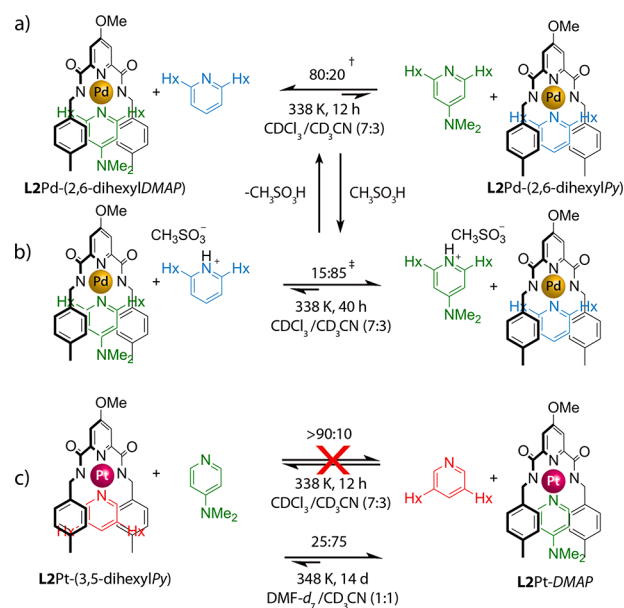
Figure 1. “Stepping” of a molecular walker with two metal-complex “feet”: L1Pd-(2,6-DMAP)¹⁴ and L1Pd-(2,6-Py).¹⁴

idine ligands about a square-planar palladium(II) center in the assembly of catenanes,¹⁰ rotaxanes,¹¹ and molecular shuttles.⁸ This complex is stabilized by the chelate effect, ensuring a square-planar metal ion remains strongly bound to the tridentate ligand, with a single additional binding site available for monodentate ligand substitution.¹² The design shown in Figure 1 exploits the preference of this class of palladium(II) and platinum(II) complexes to selectively bind N-heterocycles as a function of basicity,^{8,13} enabling their thermodynamic bias toward different ligands to be controlled by acid–base manipulations. The palladium(II) complex can be stepped back and forth between a 4-dimethylaminopyridine (DMAP) and a pyridine (Py) foothold through protonation/deprotonation and thermal activation. Throughout this process the walker should remain tethered to the track via the foot featuring the platinum(II) complex, which should have considerably higher kinetic stability under the stepping conditions. The substitution pattern of the pyridine derivatives and the kinetic stability of the metal–ligand bonds mean that altering the chemical state of the track by adding or removing protons should not automatically cause a change in the positional isomer distribution in the absence of an additional stimulus (heat in the presence of a coordinating solvent).

Operational control over discrete, well-defined stepping mechanisms is a prerequisite in the design of molecular walker systems based upon alternating stimuli-induced directional stepping² and requires careful consideration of the thermodynamics and kinetics of each step. For the bimetallic biped design L1Pd-(2,6-DMAP)¹⁴ and L1Pd-(2,6-Py),¹⁴ shown in Figure 1, the effect of varying the substitution patterns of Py and DMAP ligands on the stabilities of model metal complexes was investigated (Scheme 1).

In simple exchange experiments similar to previous studies with macrocyclic palladium(II) complexes,^{8a} L2Pd could be selectively switched between 2,6-dihexylPy and 2,6-dihexylDMAP ligands by the addition of acid or base in the presence of a coordinating solvent (Scheme 1a,b). Each of the L2Pd-2,6-disubstituted complexes was shown to be stable at both ambient and elevated temperatures (338 K) in the non-coordinating solvent CDCl₃. Conversely, some exchange of the

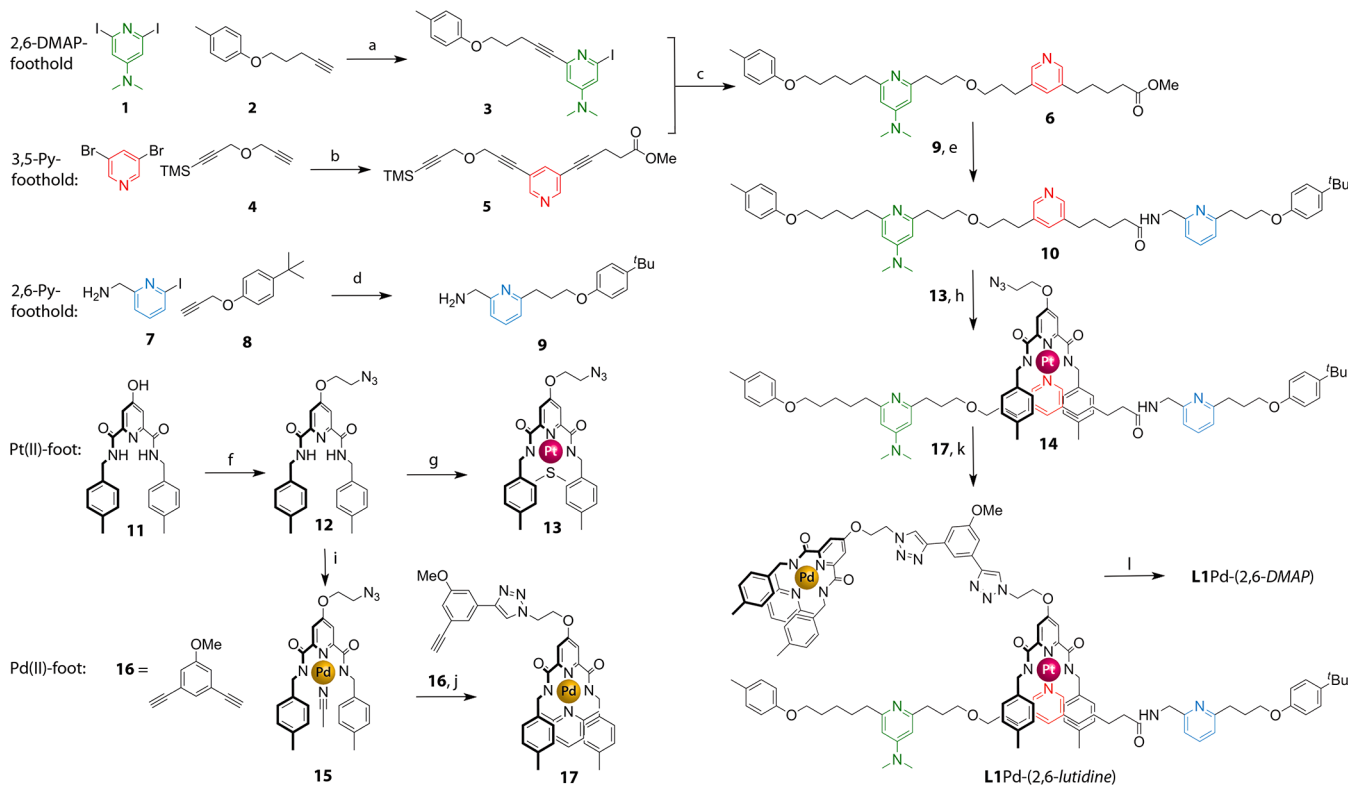
Scheme 1. Controlled Reversible Substitution of Pyridine Derivatives in Pd(II) and Pt(II) Complexes^a



^aReversible exchange of monodentate ligands¹³ in L2Pd complexes and the kinetic stability of L2Pt complexes in CDCl₃/CD₃CN (7/3) at 338 K. (a) Neutral conditions; (b) In the presence of CH₃SO₃H (1 equiv). Time required to reach equilibrium: (†) 12 h; (‡) 40 h. No exchange of 2,6-dihexyl heterocyclic ligands was observed in CDCl₃ under neutral conditions or in the presence of CH₃SO₃H, even at 338 K for 2 days. (c) System did not reach equilibrium after 12 h, in which time <10% exchange of 2,6-dihexylPy for DMAP was observed. Equilibrium was reached after 2 weeks in DMF-*d*₇/CD₃CN (1/1) at 348 K.

monodentate ligands was observed in these reactions when they were carried out in CD₃CN at room temperature (Figure S13, Supporting Information), allowing the solvent mixture to be adjusted to manipulate the exchange kinetics. Switchable kinetic control is a useful feature for producing ratchet mechanisms,^{4,9} and a CDCl₃/CD₃CN solvent mixture (7/3) was identified, for which each of the 2,6-disubstituted complexes in Scheme 1 was shown to be kinetically inert at ambient temperature (stimulus OFF). However, upon heating at 338 K (stimulus ON), 80% of the 2,6-dihexylPy coordinated to L2Pd was exchanged for 2,6-dihexylDMAP (Scheme 1a) within 12 h (the DMAP ligand forms a thermodynamically more favorable complex).¹⁵ The ligand selectivity could be reversed (Scheme 1b) by adding 1 equiv of methanesulfonic acid, where the metal's selectivity for the ligands is determined by the relative basicities of the two heterocycles.¹⁶ Although palladium(II) complexes of 3,5-disubstituted pyridines are thermodynamically preferred to the 2,6-disubstituted analogues (Figure S12, Supporting Information), their lability in the absence of external stimuli renders them unsuitable for use as feet in a molecular walker system (Figure S11, Supporting Information).

The analogous platinum(II) complex L2Pt-(3,5-dihexylPy) showed a similar thermodynamic preference for unsubstituted DMAP over Py (Figure S9, Supporting Information), although the kinetic stability of the 3,5-disubstituted pyridine complex in CDCl₃/CD₃CN (7/3) was sufficient for it to be considered relatively inert under the palladium(II) stepping conditions (<10% exchange after 12 h at 338 K; Scheme 1c). Additionally,

Scheme 2. Synthesis of the Molecular Biped Bimetallic Complex L1Pd-(2,6-DMAP)^a

^aReagents and conditions: (a) $\text{PdCl}_2(\text{PPh}_3)_2$, CuI , $\text{Et}_3\text{N}/\text{THF}$, 61%; (b) (i) 4, $\text{PdCl}_2(\text{PPh}_3)_2$, CuI , $\text{Et}_3\text{N}/\text{THF}$, 85%, (ii) methyl-4-pentynoate, $\text{PdCl}_2(\text{PPh}_3)_2$, CuI , $\text{Et}_3\text{N}/\text{THF}$, 71%; (c) (i) TBAF, $\text{THF}/\text{H}_2\text{O}$, 94%; (ii) $\text{Pd}(\text{PPh}_3)_4$, CuI , $\text{Et}_3\text{N}/\text{THF}$, 86%, (iii) H_2 , $\text{Pd}(\text{OH})_2/\text{C}$, K_2CO_3 , THF , 78%; (d) (i) Boc_2O , CH_2Cl_2 , 97%, (ii) 8, $\text{Pd}(\text{PPh}_3)_4$, CuI , $\text{Et}_3\text{N}/\text{THF}$, 88%, (iii) H_2 , $\text{Pd}(\text{OH})_2/\text{C}$, K_2CO_3 , THF , 98%, (iv) CF_3COOH , CHCl_3 , 96%; (e) (i) LiOH , $\text{MeOH}/\text{H}_2\text{O}/\text{THF}$, 97%, (ii) 9, PyBroP , DIPEA , DMF , 86%; (f) (i) 1,2-dibromoethane, K_2CO_3 , acetone, 72%, (ii) NaN_3 , NaI , DMF , 81%; (g) NaH , $\text{PtCl}_2(\text{SMe}_2)_2$, THF , 64%; (h) 13, DMF , 62%; (i) 12, $\text{Pd}(\text{OAc})_2$, CH_3CN , 84%; (j) (i) 2,6-lutidine, CH_2Cl_2 (ii) 16, DIPEA , $\text{Cu}(\text{CH}_3\text{CN})_4\cdot\text{PF}_6$, TBTA , 80% (from 15); (k) 17, DIPEA , $\text{Cu}(\text{CH}_3\text{CN})_4\cdot\text{PF}_6$, TBTA , 85%; (l) $\text{CHCl}_3/\text{CH}_3\text{CN}$ (7/3), 76%.

the steric hindrance of 2,6-dihexylpy was found to prevent any observable coordination to platinum(II) centers, enabling L2Pt complexes to perfectly discriminate between 2,6- and 3,5-disubstituted pyridine units.

The results indicated that a tethered palladium(II) complex could be made to step along a track while remaining associated with the track through a platinum(II) complex foot. Although the platinum(II) foot is employed as a fixed point of attachment in these studies, the chemistry of platinum(II) complexes may enable this foot to step through the use of orthogonal chemistries (e.g., the use of light^{13,17}).

2.2. Synthesis and Characterization of Tethered Bimetallic Transition-Metal Complex L1Pd-(2,6-DMAP).

The strategy for the assembly of bimetallic complex L1Pd-(2,6-DMAP) is shown in Scheme 2 (for synthetic procedures and characterization data see the Supporting Information). Component 6 was prepared in 41% overall yield via a series of Sonogashira cross-coupling reactions¹⁸ starting from 2,6-diiodo-4-dimethylaminopyridine (1), 3,5-dibromopyridine, and alkyne building blocks 2, 4, and 5, using standard protocols including TMS deprotection of 5 with tetrabutylammonium fluoride and subsequent hydrogenation of the alkyne groups with $\text{Pd}(\text{OH})_2/\text{C}$ (Scheme 2a–c). The final foothold of the track, compound 9, was prepared through Boc protection of 6-iodopyridin-2-ylmethylamine (7) prior to Sonogashira coupling with alkyne 8, hydrogenation, and finally Boc removal using trifluoroacetic acid (Scheme 2d). Hydrolysis of the methyl ester group of 6 using LiOH , and subsequent PyBroP mediated

amide coupling with 9, afforded the free three-foothold track 10 (Scheme 2e).

The two metal complexes 13 and 17 were prepared from the common pyridine-2,6-dicarboxamide unit 12, which was obtained in two steps by Williamson ether synthesis and subsequent azide $\text{S}_\text{N}2$ displacement from 11 (Scheme 2f). Preparation of the platinum(II) complex required deprotonation of the amide groups of 12 with NaH in THF and subsequent reaction with $\text{PtCl}_2(\text{SMe}_2)_2$ to yield the dimethyl sulfide–platinum(II) complex 13 (Scheme 2g). Selective coordination of this complex to the preferred central foothold on track 10 was achieved by stirring an equimolar solution of the two components in chloroform at room temperature for 16 h, exploiting the absolute preference of the platinum(II) complex for the 3,5-disubstitution pattern over both the 2,6-Py and 2,6-DMAP footholds (Scheme 2h).

Palladium(II) complex 15 was prepared through reaction of pyridine-2,6-dicarboxamide 12 with palladium(II) acetate in CH_3CN for 16 h to give the product as a yellow precipitate (Scheme 2i), which was converted to 17 in 80% yield (Scheme 2j) by complexation to 2,6-lutidine in CH_2Cl_2 and subsequent copper(I)-catalyzed azide–alkyne cycloaddition¹⁹ (CuAAC) using 5 equiv of dialkyne 16 (N,N -diisopropylethylamine (DIPEA), $\text{Cu}(\text{CH}_3\text{CN})_4\cdot\text{PF}_6$, tris[(1-benzyl-1*H*-1,2,3-triazol-4-yl)methyl]amine (TBTA), 12 h).

The coupling of the palladium(II) and platinum(II) complexes (17 and 14, respectively) required selective intramolecular coordination of the palladium(II) center to the

preferred N-heterocycle binding site in addition to the formation of the covalent bond between the two “legs” of the walker using the CuAAC reaction. To achieve this, an equimolar mixture of **17** and **14** was subjected to the azide–alkyne cycloaddition conditions to afford the bimetallic intermediate LIPd-(2,6-lutidine) (Scheme 2k), demonstrating that CuAAC “click” reactions are practical synthetic ligation tools in the presence of transition-metal complexes and multiple metal binding sites, despite the potential for pyridines to bind Cu(I). Adjusting the reaction concentration to favor intramolecular coordination of the 2,6-DMAP foothold, LIPd-(2,6-lutidine) was subjected to the conditions optimized in the model exchange experiments ($\text{CHCl}_3/\text{CH}_3\text{CN}$ (7/3), 0.16 mM, 338 K, 14 h, Scheme 1a), exploiting both the disparate ligand strengths of the free 2,6-lutidine and the 2,6-DMAP/Py footholds of the track and the kinetic stability of the Pt-(3,5-Py) complex, to form the bimetallic complex LIPd in 76% isolated yield after silica column chromatographic purification (Scheme 2l). Electrospray mass spectrometry confirmed the isolated product constitution as LIPd with mass peaks at m/z 2225.6 and 2247.9 corresponding to the $[\text{M} + \text{H}]^+$ and $[\text{M} + \text{Na}]^+$ ions, respectively, with isotopic distributions in agreement with theoretical predictions (Figure S20a, Supporting Information).

Slow evaporation of a solution of the closely related bimetallic walker–track complex **18** (Figure 2a) in $\text{CHCl}_3/$

EtOH afforded single crystals suitable for X-ray diffraction analysis.²⁰ The solid-state structure (Figure 2b) confirms the coordination of the palladium(II) moiety to the DMAP foothold. All metal–ligand bonds lie within the expected ranges and are similar for the palladium(II) and platinum(II) complexes, both of which adopt distorted-square-planar coordination geometries (Figure 2b). The tolyl rings of the dicarboxamide motifs do not participate in π – π stacking with the DMAP or Py footholds of the track, instead adopting conformations similar to those observed previously for related macrocyclic ligands.^{8a,11a} The 3,5-ditriazoloanisole linker unit is almost coplanar, with the three central hydrogen atoms engaged in intermolecular hydrogen-bond interactions with the oxygen atom of a carbonyl group of an adjacent palladium(II)-containing motif ($[\text{C}–\text{H}\cdots\text{O}]$ distances 2.38, 2.39, and 2.39 Å).

¹H NMR spectroscopy (Figure 3b) of the isolated complex LIPd confirms that it is a single positional isomer with the palladium(II) complex of the biped coordinated solely to the 2,6-DMAP foothold, analogous to the case for compound **18**. A comparison between the spectra of free track **10** (Figure 3a) and LIPd-(2,6-DMAP) in CD_2Cl_2 shows the expected upfield shifts of the signals of both the 2,6-DMAP ($\Delta\delta(\text{H}_i) = -0.20$ ppm and $\Delta\delta(\text{H}_k) = -0.18$ ppm) and the 3,5-Py groups ($\Delta\delta(\text{H}_r) = -0.88$ ppm, $\Delta\delta(\text{H}_s) = -0.29$ ppm, and $\Delta\delta(\text{H}_t) = -0.45$ ppm), while the resonances of the 2,6-Py foothold ($\text{H}_{\text{aa-cc}}$) and those relating to the adjacent methylene (H_z) occur at almost identical values in both species.

2.3. Protonation-Driven Switching. In accordance with model studies, in the absence of acid the palladium(II) complex of LIPd-(2,6-DMAP) was thermodynamically stable when heated in $\text{CDCl}_3/\text{CD}_3\text{CN}$ (7/3) at 338 K.²¹ Upon addition of 1 equiv of methanesulfonic acid to a pure sample at room temperature, the ¹H NMR spectrum showed significant broadening in the 2,6-Py resonances ($\text{H}_{\text{aa-cc}}$) but no discernible change in either the 2,6-DMAP (H_{ik}) or the 3,5-Py signals (H_{rt}), indicating that protonation of the 2,6-Py foothold had occurred but no positional isomerization had taken place (Scheme 3). No changes were observed after 30 h at room temperature, indicating that the transition-metal complexes are kinetically locked in the presence of acid under ambient conditions.

Stepping of the LIPd complex was only observed at 338 K in the presence of 1 equiv of acid. The operation was monitored by ¹H NMR spectroscopy and shown to reach equilibrium within 40 h, after which no further exchange was observed. The reaction mixture was diluted with toluene by a factor of 2, and the solvents were removed gradually under reduced pressure to ensure a consistently low concentration of the machine with respect to the coordinating solvent, CH_3CN .²² The crude residue was deprotonated (K_2CO_3 , CH_2Cl_2 , 30 min) and the sample analyzed by ¹H NMR to reveal an equilibrium 15:85 distribution of LIPd-(2,6-DMAP) and LIPd-(2,6-Py) (see Figure S19, Supporting Information).

The neutral positional isomers obtained were readily separated by preparative thin-layer chromatography to give pure kinetically stable samples of both LIPd-(2,6-Py) (major product) and LIPd-(2,6-DMAP) (minor product). The ¹H NMR spectrum of the former is shown in Figure 3c, while the latter precisely matched that of the original sample of LIPd-(2,6-DMAP). After operation, the resonances of the 2,6-DMAP foothold (H_{ik}) were found to have shifted downfield ($\Delta\delta(\text{H}_i) = 0.17$ ppm and $\Delta\delta(\text{H}_k) = 0.18$ ppm), resembling the

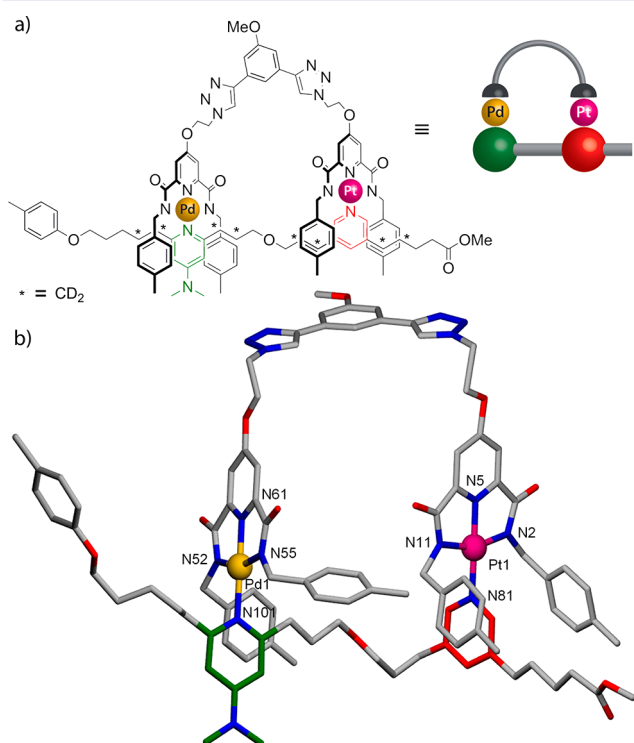


Figure 2. X-ray crystal structure of bimetallic walker-track complex **18**: (a) chemical structure; (b) framework representation of the X-ray crystal structure. Hydrogen and deuterium atoms and solvent molecules are omitted for clarity. Nitrogen atoms are shown in blue, oxygen atoms in red, the palladium atom in gold, the platinum atom in pink, and carbon atoms in gray (DMAP and pyridine carbon atoms are shown in green and red, respectively). Selected bond lengths (Å) and angles (deg): Pd1–N52, 2.027; Pd1–N55, 1.939; Pd1–N61, 2.034; Pd1–N101, 2.113; Pt1–N2, 2.021; Pt1–N5, 1.925; Pt1–N11, 2.027; Pt1–N81, 2.043; N52–Pd1–N61, 160.3; N11–Pt1–N2, 160.6; N55–Pd1–N101, 178.1; N5–Pt1–N81, 179.0.

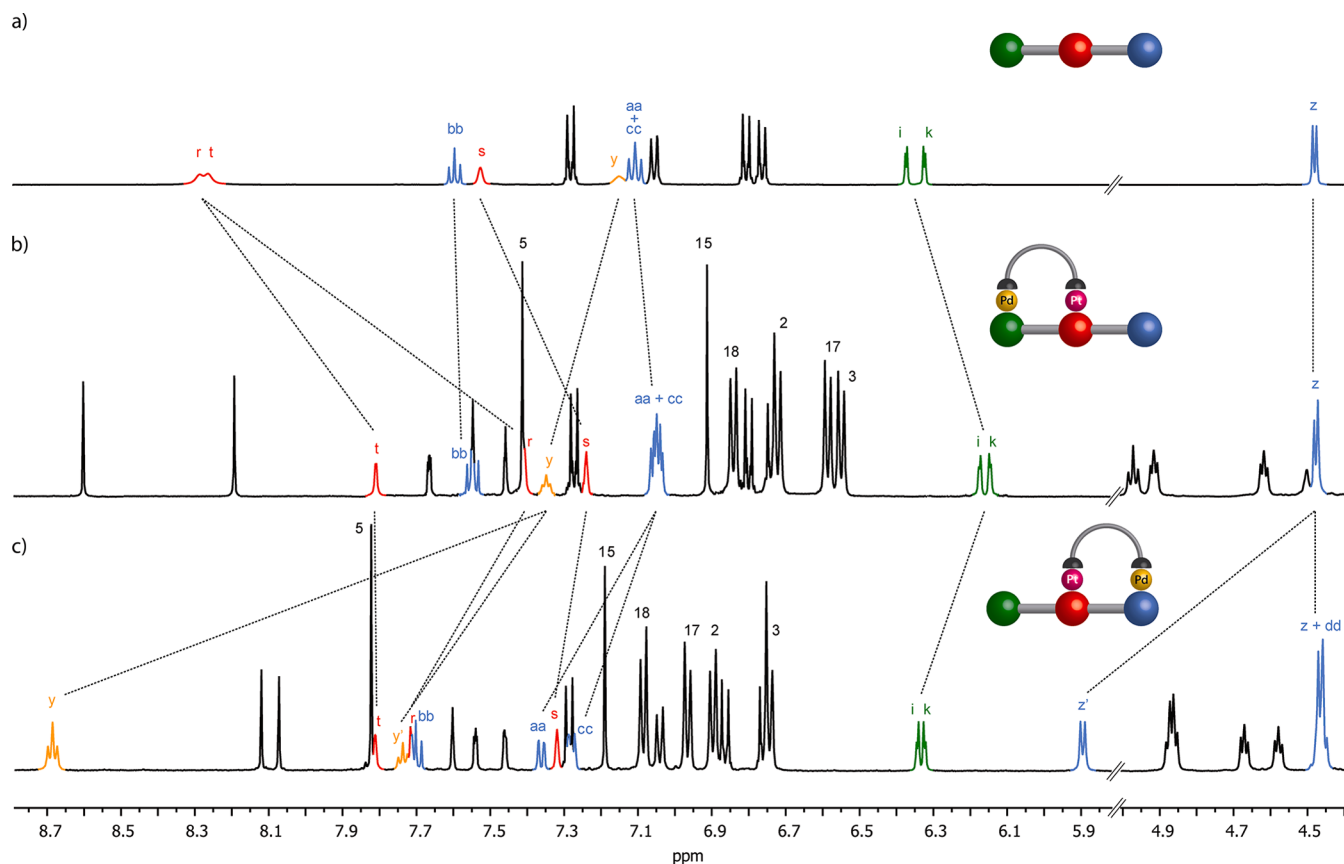
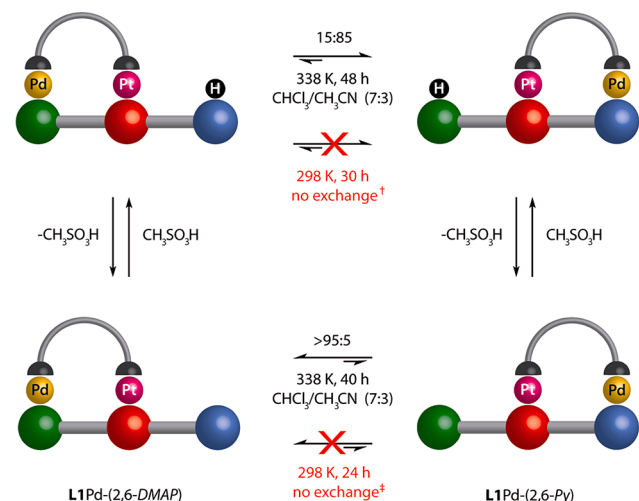


Figure 3. ^1H NMR spectra (500 MHz, CD_2Cl_2 , 298 K) of the two positional isomers of the bimetallic complex **L1Pd** and the free track for comparison: (a) track **10**; (b) **L1Pd**-(2,6-DMAP); (c) **L1Pd**-(2,6-Py). The lettering in the figure refers to the assignments shown in Figure 1.

Scheme 3. Stepping of a Pd(II)/Pt(II)-Complexed Molecular Biped^a



^aLegend: (†) no exchange after 30 h at 298 K in $\text{CDCl}_3/\text{CD}_3\text{CN}$ (7/3) with $\text{CH}_3\text{SO}_3\text{H}$ (1 equiv), <5% exchange in $\text{CDCl}_3/\text{CD}_3\text{CN}$ after 30 h at 338 K with no $\text{CH}_3\text{SO}_3\text{H}$; (‡) No exchange observed after 24 h at 298 K in $\text{CDCl}_3/\text{CD}_3\text{CN}$ (7/3).

noncomplexed 2,6-DMAP foothold in the free track, **10** (Figure 3a). Similarly, the 2,6-Py signals ($H_{\text{aa-cc}}$) show shifts ($\Delta\delta(H_{\text{aa}}) = 0.31$ ppm, $\Delta\delta(H_{\text{bb}}) = 0.16$ ppm, and $\Delta\delta(H_{\text{cc}}) = 0.24$ ppm) in accordance with the equivalent resonances in the model exchange experiment (Scheme 1b; see Figure S5, Supporting

Information, for NMR). Interestingly, upon enclosing the amide bond of the track within the macrocycle of **L1Pd**-(2,6-Py), two separate signals can be seen for both the amide ($H_{\text{y/y'}}$) and the adjacent methylene protons ($H_{\text{z/z'}}$) as a result of *cis*-/*trans*-amide isomers ($H_{\text{y+z}}$, major isomer, $H_{\text{y'+z'}}$, minor isomer). Electrospray mass spectrometry of the product showed identical peaks (m/z 2226.0 $[\text{M} + \text{H}]^+$ and 2248.0 $[\text{M} + \text{Na}]^+$) with isotopic distribution matching those observed for **L1Pd**-(2,6-DMAP) (see Figure S20b, Supporting Information), supporting the identity of the new product as the positional isomer **L1Pd**-(2,6-Py).

2.4. Deprotonation-Driven Switching. A sample of the neutralized 15:85 crude mixture of **L1Pd**-(2,6-DMAP) and **L1Pd**-(2,6-Py) from the protonation-driven stepping experiment was heated at 338 K in $\text{CDCl}_3/\text{CD}_3\text{CN}$ (7/3). After 24 h at 338 K, the ratio of the positional isomers had changed to >95:5 in favor of **L1Pd**-(2,6-DMAP), while in an identical sample left at room temperature for the same period, no change in positional isomer ratio was observed. The ratio observed at equilibration at 338 K is in accordance with the previous neutral stepping experiment (Figure S18, Supporting Information), demonstrating an equilibrium distribution overwhelmingly in favor of **L1Pd**-(2,6-DMAP) in the absence of acid, confirming the reversibility of the switching mechanism. These experiments illustrate that the coordination chemistry of the palladium(II) foot allows the walker–track system to be locked in a thermodynamically unfavorable positional isomer distribution between the two footholds, enabling ratcheting of the biped unit away from its equilibrium state and, in principle, such a mechanism to be used to bring about directional walking

of a molecular biped with a palladium(II)-coordinated foot on an extended track.

3. CONCLUSIONS

Nature boasts a plethora of molecular-level systems in which the thermodynamics and kinetics of binding events can be rapidly and systematically controlled via manipulation of hydrogen-bonding and electrostatic interactions to bring about directional molecular-level motion. The design of synthetic mimics of these systems is particularly difficult because of the weak and ephemeral nature of such binding events. Metal coordination motifs provide a potential alternative to controlled molecular-level motion by exploiting the kinetics and thermodynamics of ligand binding events. We have described an acid–base switchable palladium(II)/platinum(II) bimetallic system in which one of two transition-metal complexes can be selectively labilized and stepped in either direction between two different binding sites and kinetically relocked with a high degree of positional discrimination. Such systems should prove useful in the development of switchable, metastable components for advanced molecular machinery, most notably linear molecular motors in the form of synthetic small-molecule walkers.

■ ASSOCIATED CONTENT

Supporting Information

Text, figures, a table, giving experimental procedures and spectral data for all compounds and details of the X-ray analysis of **18** and the associated CIF file. This material is available free of charge via the Internet at <http://pubs.acs.org>.

■ AUTHOR INFORMATION

Corresponding Author

David.Leigh@manchester.ac.uk

Notes

The authors declare no competing financial interest.

■ ACKNOWLEDGMENTS

We thank Dr. Paul J. Lusby and Dr. James D. Crowley for useful discussions, the Engineering and Physical Sciences Research Council (EPSRC) for funding, and the EPSRC National Mass Spectrometry Service Centre (Swansea, U.K.) for high-resolution mass spectrometry. We are grateful for postdoctoral fellowships to J.E.B. (Swiss National Science Foundation), V.B. (Marie Curie Intra European Fellowship within the 7th European Framework Program), B.A.B. (Marie Curie International Incoming Fellowship within the 7th European Framework Program), R.C. (Fundación Ramón Areces), and D.M.D. (Deutsche Akademie der Naturforscher Leopoldina (BMBF LPD 9901/8-166) and Peter und Traudl Engelhorn-Stiftung).

■ REFERENCES

(1) (a) von Delius, M.; Geertsema, E. M.; Leigh, D. A. *Nat. Chem.* **2010**, *2*, 96–101. (b) von Delius, M.; Geertsema, E. M.; Leigh, D. A.; Tang, D.-T. *J. Am. Chem. Soc.* **2010**, *132*, 16134–16145. (c) Barrell, M. J.; Campaña, A. G.; von Delius, M.; Geertsema, E. M.; Leigh, D. A. *Angew. Chem., Int. Ed.* **2011**, *50*, 285–290. (d) Perl, A.; Gomez-Casado, A.; Thompson, D.; Dam, H. H.; Jonkheijm, P.; Reinhoudt, D. N.; Huskens, J. *Nat. Chem.* **2011**, *3*, 317–322. (e) Campaña, A. G.; Carbone, A.; Chen, K.; Dryden, D. T. F.; Leigh, D. A.; Lewandowska, U.; Mullen, K. M. *Angew. Chem., Int. Ed.* **2012**, *51*, 5480–5483. (f) Kovaříček, P.; Lehn, J.-M. *J. Am. Chem. Soc.* **2012**, *134*, 9446–9455.

(g) Campaña, A. G.; Leigh, D. A.; Lewandowska, U. *J. Am. Chem. Soc.* **2013**, *135*, 8639–8645.

(2) (a) von Delius, M.; Leigh, D. A. *Chem. Soc. Rev.* **2011**, *40*, 3656–3676. (b) Qu, D.-H.; Tian, H. *Chem. Sci.* **2013**, *4*, 3031–3035.

(3) (a) Vale, R. D. *Cell* **2003**, *112*, 467–480. (b) Schliwa, M.; Woehlke, G. *Nature* **2003**, *422*, 759–765. (c) Mallik, R.; Gross, S. P. *Curr. Biol.* **2004**, *14*, R971–R982. (d) Amos, L. A. *Cell. Mol. Life Sci.* **2008**, *65*, 509–515.

(4) Kay, E. R.; Leigh, D. A.; Zerbetto, F. *Angew. Chem., Int. Ed.* **2007**, *46*, 72–191.

(5) Changes in metal oxidation state can alter coordination geometry preferences, which have proven to be effective means to generate intramolecular ligand rearrangements. See, for example: (a) Zahn, S.; Canary, J. W. *Angew. Chem., Int. Ed.* **1998**, *37*, 305–307. (b) He, Z.; Colbran, S. B.; Craig, D. C. *Chem. Eur. J.* **2003**, *9*, 116–129. (c) Fabbri, L.; Foti, F.; Patroni, S.; Pallavicini, P.; Taglietti, A. *Angew. Chem., Int. Ed.* **2004**, *43*, 5073–5077. (d) Amendola, V.; Dallacosta, C.; Fabbri, L.; Monzani, E. *Tetrahedron* **2008**, *64*, 8318–8323. (e) Kuwamura, N.; Kitano, K.; Hirotsu, M.; Nishioka, T.; Teki, Y.; Santo, R.; Ichimura, A.; Hashimoto, H.; Wright, L. J.; Kinoshita, I. *Chem. Eur. J.* **2011**, *17*, 10708–10715. For examples of redox-driven translocation of metal ions, see: (f) Zelikovich, L.; Libman, J.; Shanzer, A. *Nature* **1995**, *374*, 790–792. (g) Amendola, V.; Fabbri, L.; Mangano, C.; Pallavicini, P. *Acc. Chem. Res.* **2001**, *34*, 488–493. (h) Champin, B.; Mobian, P.; Sauvage, J.-P. *Chem. Soc. Rev.* **2007**, *36*, 358–366. (i) Colasson, B.; Le Poul, N.; Le Mest, Y.; Reinaud, O. *J. Am. Chem. Soc.* **2010**, *132*, 4393–4398. (j) Murahashi, T.; Shirato, K.; Fukushima, A.; Takase, K.; Suenobu, T.; Fukuzumi, S.; Ogoshi, S.; Kurosawa, H. *Nat. Chem.* **2012**, *4*, 52–58. For the mechanical movement of macrocycle-bound metal ions using redox processes, see: (k) Livoreil, A.; Dietrich-Buchecker, C. O.; Sauvage, J.-P. *J. Am. Chem. Soc.* **1994**, *116*, 9399–9400. (l) Cárdenas, D. J.; Livoreil, A.; Sauvage, J.-P. *J. Am. Chem. Soc.* **1996**, *118*, 11980–11981. (m) Gaviña, P.; Sauvage, J.-P. *Tetrahedron Lett.* **1997**, *38*, 3521–3524. (n) Livoreil, A.; Sauvage, J.-P.; Armaroli, N.; Balzani, V.; Flamigni, L.; Ventura, B. *J. Am. Chem. Soc.* **1997**, *119*, 12114–12124. (o) Armaroli, N.; Balzani, V.; Collin, J.-P.; Gaviña, P.; Sauvage, J.-P.; Ventura, B. *J. Am. Chem. Soc.* **1999**, *121*, 4397–4408. (p) Raehm, L.; Kern, J.-M.; Sauvage, J.-P. *Chem. Eur. J.* **1999**, *5*, 3310–3317. (q) Weber, N.; Hamann, C.; Kern, J.-M.; Sauvage, J.-P. *Inorg. Chem.* **2003**, *42*, 6780–6792. (r) Poleschak, I.; Kern, J.-M.; Sauvage, J.-P. *Chem. Commun.* **2004**, 474–476. (s) Létinois-Halbes, U.; Hanss, D.; Beierle, J. M.; Collin, J.-P.; Sauvage, J.-P. *Org. Lett.* **2005**, *7*, 5753–5756. (t) Bonnet, S.; Collin, J.-P.; Koizumi, M.; Mobian, P.; Sauvage, J.-P. *Adv. Mater.* **2006**, *18*, 1239–1250. (u) Durola, F.; Sauvage, J.-P. *Angew. Chem., Int. Ed.* **2007**, *46*, 3537–3540. (v) Collin, J.-P.; Durola, F.; Lux, J.; Sauvage, J.-P. *Angew. Chem., Int. Ed.* **2009**, *47*, 8532–8535. (w) Periyasamy, G.; Collin, J.-P.; Sauvage, J.-P.; Levine, R. D.; Remacle, F. *Chem. Eur. J.* **2009**, *15*, 1310–1313. (x) Durola, F.; Lux, J.; Sauvage, J.-P. *Chem. Eur. J.* **2009**, *15*, 4124–4134. (y) McNitt, K. A.; Parimal, K.; Share, A. I.; Fahrenbach, A. C.; Witlicki, E. H.; Pink, M.; Bediako, D. K.; Plaisier, C. L.; Le, N.; Heeringa, L. P.; Griend, D. A. V.; Flood, A. H. *J. Am. Chem. Soc.* **2009**, *131*, 1305–1313. (z) Durot, S.; Reviriego, F.; Sauvage, J.-P. *Dalton Trans.* **2010**, *39*, 10557–10570.

(6) For examples of large-amplitude molecular motions brought about by reversible binding, see: (a) Barboiu, M.; Vaughan, G.; Kyritsakas, N.; Lehn, J.-M. *Chem. Eur. J.* **2003**, *9*, 763–769. (b) Guenet, A.; Graf, E.; Kyritsakas, N.; Hosseini, M. W. *Inorg. Chem.* **2010**, *49*, 1872–1883. (c) Haberhauer, G. *Angew. Chem., Int. Ed.* **2010**, *49*, 9286–9289. (d) Mirtschin, S.; Slabon-Turski, A.; Scopelliti, R.; Velders, A. H.; Severin, K. *J. Am. Chem. Soc.* **2010**, *132*, 14004–14005. (e) Haberhauer, G. *Angew. Chem., Int. Ed.* **2011**, *50*, 6415–6418. (f) Kilbas, B.; Mirtschin, S.; Scopelliti, R.; Severin, K. *Chem. Sci.* **2012**, *3*, 701–704. For examples of “molecular muscle” rotaxanes that employ switchable Cu(I)/Zn(II) binding, see: (g) Jiménez, M. C.; Dietrich-Buchecker, C.; Sauvage, J.-P. *Angew. Chem., Int. Ed.* **2000**, *39*, 3284–3287. (h) Collin, J.-P.; Dietrich-Buchecker, C.; Gaviña, P.; Jimenez-Molero, M. C.; Sauvage, J.-P. *Acc. Chem. Res.* **2001**, *34*, 477–487. For an example of large-amplitude molecular motion achieved by

solvent-mediated hydrogen bond manipulation in transition-metal–porphyrin systems, see: (i) Guenet, A.; Graf, E.; Kyritsakas, N.; Hosseini, M. W. *Chem. Eur. J.* **2011**, *17*, 6443–6452.

(7) For examples of photodriven molecular machines, see: (a) Koumura, N.; Geertsema, E. M.; van Gelder, M. B.; Meetsma, A.; Feringa, B. L. *J. Am. Chem. Soc.* **2002**, *124*, 5037–5051. (b) Kay, E. R.; Leigh, D. A. *Nature* **2006**, *440*, 286–287. (c) Saha, S.; Stoddart, J. F. *Chem. Soc. Rev.* **2007**, *36*, 77–92. For examples of a photodriven motion of transition-metal-based machines, see: (d) Mobian, P.; Kern, J.-M.; Sauvage, J.-P. *Angew. Chem., Int. Ed.* **2004**, *43*, 2392–2395. (e) Bonnet, S.; Collin, J.-P. *Chem. Soc. Rev.* **2008**, *37*, 1207–1217. (f) Balzani, V.; Bergamini, G.; Marchioni, F.; Ceroni, P. *Coord. Chem. Rev.* **2006**, *250*, 1254–1266.

(8) For Pd(II)-based molecular shuttles with macrocycle positional changes driven by acid–base changes, see: (a) Crowley, J. D.; Leigh, D. A.; Lusby, P. J.; McBurney, R. T.; Perret-Aebi, L.-E.; Petzold, C.; Slawin, A. M. Z.; Symes, M. D. *J. Am. Chem. Soc.* **2007**, *129*, 15085–15090. (b) Leigh, D. A.; Lusby, P. J.; McBurney, R. T.; Symes, M. D. *Chem. Commun.* **2010**, *46*, 2382–2384.

(9) (a) Chatterjee, M. N.; Kay, E. R.; Leigh, D. A. *J. Am. Chem. Soc.* **2006**, *128*, 4058–4073. (b) Serreli, V.; Lee, C.-F.; Kay, E. R.; Leigh, D. A. *Nature* **2007**, *445*, 523–527. (c) Alvarez-Pérez, M.; Goldup, S. M.; Leigh, D. A.; Slawin, A. M. Z. *J. Am. Chem. Soc.* **2008**, *130*, 1836–1838. (d) Carlone, A.; Goldup, S. M.; Lebrasseur, N.; Leigh, D. A.; Wilson, A. J. *J. Am. Chem. Soc.* **2012**, *134*, 8321–8323.

(10) (a) Fuller, A.-M. L.; Leigh, D. A.; Lusby, P. J.; Slawin, A. M. Z.; Walker, D. B. *J. Am. Chem. Soc.* **2005**, *127*, 12612–12619. (b) Leigh, D. A.; Lusby, P. J.; Slawin, A. M. Z.; Walker, D. B. *Chem. Commun.* **2005**, 4919–4921.

(11) (a) Fuller, A.-M.; Leigh, D. A.; Lusby, P. J.; Oswald, I. D. H.; Parsons, S.; Walker, D. B. *Angew. Chem., Int. Ed.* **2004**, *43*, 3914–3918. (b) Furusho, Y.; Matsuyama, T.; Takata, T.; Moriuchi, T.; Hirao, T. *Tetrahedron Lett.* **2004**, *45*, 9593–9597. (c) Fuller, A.-M. L.; Leigh, D. A.; Lusby, P. J. *Angew. Chem., Int. Ed.* **2007**, *46*, 5015–5019. (d) Hung, W.-C.; Wang, L.-Y.; Lai, C.-C.; Liu, Y.-H.; Peng, S.-M.; Chiu, S.-H. *Tetrahedron Lett.* **2009**, *50*, 267–270. (e) Fuller, A.-M. L.; Leigh, D. A.; Lusby, P. J. *J. Am. Chem. Soc.* **2010**, *132*, 4954–4959.

(12) Slagt, M. Q.; van Zwieten, D. A. P.; Moerkerk, A. J. C. M.; Klein Gebbink, R. J. M.; van Koten, G. *Coord. Chem. Rev.* **2004**, *248*, 2275–2282.

(13) (a) Pike, S. J.; Lusby, P. J. *Chem. Commun.* **2010**, *46*, 8338–8340. (b) South, C. R.; Leung, K. C.-F.; Lanari, D.; Stoddart, J. F.; Weck, M. *Macromolecules* **2006**, *39*, 3738–3744.

(14) The italicized suffixes *-DMAP*, *-Py*, and *-2,6-lutidine* denote that the monodentate ligand is coordinated to the aforementioned metal.

(15) For exchange of various 4-substituted pyridine ligands at the fourth coordination site of Pd–pincer complexes, see: (a) van Manen, H.-J.; Nakashima, K.; Shinkai, S.; Kooijman, H.; Spek, A. L.; van Veggel, F. C. J. M.; Reinhoudt, D. N. *Eur. J. Inorg. Chem.* **2000**, 2533–2540. (b) Yount, W. C.; Loveless, D. M.; Craig, S. L. *J. Am. Chem. Soc.* **2005**, *127*, 14488–14496.

(16) For proton-driven ligand exchange of lutidine coordinated to Pd(II), see: (a) Hamann, C.; Kern, J.-M.; Sauvage, J.-P. *Dalton Trans.* **2003**, 3770–3775. For proton-driven exchange of various amines within copper-coordinated imine ligands, see: (b) Nitschke, J. R.; Schultz, D.; Bernardinelli, G.; Gérard, D. *J. Am. Chem. Soc.* **2004**, *126*, 16538–16543. (c) Schultz, D.; Nitschke, J. R. *Proc. Natl. Acad. Sci. U.S.A.* **2005**, *102*, 11191–11195. (d) Nitschke, J. R. *Acc. Chem. Res.* **2007**, *40*, 103–112.

(17) (a) Yamashita, K.-i.; Kawano, M.; Fujita, M. *J. Am. Chem. Soc.* **2007**, *129*, 1850–1851. (b) Yamashita, K.-i.; Sato, K.-i.; Kawano, M.; Fujita, M. *New J. Chem.* **2009**, *33*, 264–270.

(18) Sonogashira, K.; Tohda, Y.; Hagihara, N. *Tetrahedron Lett.* **1975**, *16*, 4467–4470.

(19) Kolb, H. C.; Finn, M. G.; Sharpless, K. B. *Angew. Chem., Int. Ed.* **2001**, *40*, 2004–2021.

(20) Crystal data for **18**·2EtOH: yellow prism, 0.03 × 0.20 × 0.20 mm, $M_w = 2068.70$, $C_{101}H_{103}D_{16}N_{15}O_{13}PdPt$, triclinic, space group $P\bar{1}$, $a = 14.238(4)$ Å, $b = 18.939(5)$ Å, $c = 19.681(5)$ Å, $\alpha = 104.533(6)^\circ$, β

$= 96.912(8)^\circ$, $\gamma = 94.763(4)^\circ$, $V = 5064(2)$ Å³, $Z = 2$, $D_c = 1.357$ g/cm³, Mo $K\alpha$ radiation (graphite monochromator, $\lambda = 0.71075$ Å), $\mu = 1.624$ mm^{−1}, $T = 93(2)$ K, $F(000) = 2116$, 32421 data (17832 unique, $R_{int} = 0.055$, $2.16 < \theta < 25.3$), 1168 parameters, 35 restraints, $R = 0.1041$ ($I_o > 2\sigma(I_o)$), $R_w = 0.3374$ (all reflections), $S = 1.23$.

(21) <5% exchange to the alternative positional isomer observed after 30 h.

(22) When the concentration of **L1**Pd was increased in a coordinating solvent, a significant degree of intermolecular ligand exchange was observed, leading to the formation of polymeric material. In order to avoid this, when removing the solvent, the temperature was maintained below 40 °C, and the concentration with respect to coordinating solvent was never increased above the exchange reaction concentration (0.1 mM).